Journal of Materials Chemistry B

RSC Publishing

PAPER

View Article Online
View Journal | View Issue

Zinc oxide–multiwalled carbon nanotubes hybrid nanocomposite based urea biosensor†

Cite this: *J. Mater. Chem. B*, 2013, **1**, 6392

Manvi Tak,[a] Vinay Gupta[a] and Monika Tomar*[b]

An efficient matrix comprising a hybrid nanocomposite of zinc oxide (ZnO) and multiwalled carbon nanotubes (MWCNTs) has been synthesised on indium tin oxide coated glass slides (ITO/Glass) using a chemical route deposition technique for the realization of an efficient urea biosensor. Urease (Urs) was used as the specific enzyme for urea detection and was physically immobilized over the surface of the hybrid nanocomposite matrix based (ZnO–MWCNT/ITO) electrode. The fabricated Urs/ZnO–MWCNT/ITO bioelectrode was characterized using electrochemical impedance spectroscopy (EIS) and cyclic voltammetric (CV) techniques. The nanocomposite based bioelectrode *i.e.* Urs/ZnO–MWCNT/ITO exhibits enhanced biosensing response characteristics as compared to that of the bare ZnO based (Urs/ZnO/ITO) bioelectrode. The prepared bioelectrode (Urs/ZnO–MWCNT/ITO) exhibits a very high sensitivity of about 43.02 μA mM^{-1} cm^{-2} and a long shelf-life of more than 4 months (>16 weeks). The low Michaelis–Menten parameter (K_m) value, only 0.85 mM, indicates high affinity of the immobilized urease on the surface of hybrid nanocomposite matrix towards its analyte (urea). The obtained results in the present study are encouraging and will pave the way towards the realization of an efficient urea biosensor.

Received 4th July 2013
Accepted 26th September 2013

DOI: 10.1039/c3tb20935k

www.rsc.org/MaterialsB

1. Introduction

Urea is a the vital biomolecule that is present in nature and its estimation is of utmost relevance not only for clinical purposes but also from environmental perspectives.[1,2] The annual world production of urea is about 100 million metric tonnes, the majority of which is used as fertilizers.[3] The use of excessive nitrogen fertilizers may result in increased birth rate, life-span and fitness of certain pests which pose major threats to annual food production.[3] Urea may also be responsible for reductions in soil pH thus hampering its natural fertility which results in lower productivity of food grains.[3] In the human body urea is present in specific quantities in various pathological fluids such as blood, serum and urine.[4] If the level of urea in human blood/serum is abnormal, *i.e.* above or below physiological range (8–20 mg dl^{-1}), it can lead to diseases like renal failure, hepatic failure, nephritic syndrome, cachexia, urinary tract obstruction, dehydration, shock, burns and gastrointestinal problems, *etc.*[4–6] Hence, the development of robust and reliable instrumentation for continuous monitoring of this vital biomolecule in human serum/blood is important. In this context, electrochemical biosensors have recently gained much attention as they provide easy and quick operation, good accuracy, high sensitivity and selectivity for estimation of biomolecules.[7,8]

Several matrices such as conducting polymers,[8–10] non-conducting polymers,[11,12] metal oxides,[13] metal nanoparticles,[14] *etc.* prepared using various techniques including sol–gel technique,[15,16] LB technique,[17] chemical deposition[18,19] and sputtering[20] have been utilized for fabricating urea biosensors.

Metal oxides nowadays have gained much popularity as matrices from the biosensing perspective due to their well-known features like good chemical stability, chemical inertness, fast electron transfer properties, negligible swelling in both aqueous and non-aqueous media.[21,22] ZnO is one of the most important functional materials for its versatile applications, which is attributed to its distinguished properties such as wide direct band gap, large exciton binding energy, excellent chemical and thermal stability, and good piezoelectric properties.[23,24] In the field of biosensing, ZnO has gained much attention because of its unique properties like high catalytic efficiency, strong adsorption ability, bio-compatibility and high isoelectric point (IEP $\sim$ 9.5) which is important for immobilization of enzymes like urease having low IEP ($\sim$5.0) *via* physical adsorption.[25] However, the sensitivity and stability of ZnO based biosensors are relatively better than those of other matrices such as conducting polymers, but are still limited for commercial device applications.[26] Nowadays carbon based materials such as graphene oxide (GO) and carbon nanotubes (CNTs) have been in great demand because of their excellent chemical and physical properties. Recently, Zhou *et al.* have reported the fabrication of an ultrasensitive electrochemical

[a]*Department of Physics and Astrophysics, University of Delhi, Delhi 110007, India*
[b]*Department of Physics, Miranda House, University of Delhi, Delhi 110007, India. E-mail: monikatomar@gmail.com; Tel: +91 9871346452*

† Electronic supplementary information (ESI) available. See DOI: 10.1039/c3tb20935k

sensor utilizing ionic liquid functionalized graphene oxide (GO-IL) and gold nanoparticles (AuNPs) based electrode for the detection of mercury (Hg^{2+}) ions which are responsible for toxicity in water.[27] The fabricated biosensor shows promising biosensing results such as very wide detection range and low detection limit. Another work based on highly sensitive and selective voltammetric detection of mercury(II) using an ITO electrode modified with 5-methyl-2-thiouracil, graphene oxide and gold nanoparticles has also been reported by Zhou *et al.*[28] again showing very good biosensing results thus highlighting the usefulness of graphene oxide based composites in the field of biosensing. Recently, multiwalled carbon nanotubes (MWCNTs) have also gained special interest due to their unique electronic, mechanical, and structural characteristics and are promising for immobilization of proteins due to their significant surface area, excellent electrical conductivity and good chemical stability.[29] The basic characteristics of biosensors like selectivity, sensitivity and stability could be improved utilizing excellent properties of two materials such as ZnO and MWCNTs in the form of a hybrid composite matrix. A few reports in literature are available on the study of ZnO–MWCNT hybrid nanocomposites for biosensor applications; for instance, one report is based on the detection of hydroxylamine (NH_2OH) using an electrochemical sensor based on electrodeposition of porous ZnO nanofilms onto a carbon nanotube film modified electrode.[30] Another report is based on the detection of hydrazine (N_2H_4) using an electrochemical sensor utilizing a carbon nanotube-wired ZnO nanoflower-modified electrode.[31] Palanisamy *et al.* has reported fabrication of an amperometric hydrogen peroxide biosensor using a composite of MWCNTs and zinc oxide, Wang *et al.* has fabricated a lactate biosensor using ZnO nanoparticles and MWCNTs, and an electroluminescence based lactate biosensor utilizing ZnO nanoparticles decorated MWCNTs has been reported.[32–34] However, to the best of our knowledge no attempt has been made towards realization of an efficient urea biosensor utilizing a hybrid composite matrix of ZnO and MWCNTs.

There have been reports in the past on amperometric urea biosensors using a dual enzyme based technique which involves oxidation of NH_4^+ ions formed during hydrolysis of urea in the presence of urease to produce nitrogen molecules with the help of a second enzyme, but this method suffers from complex sensor structure and higher sensor cost. The second most popular urea detection technique is by using an ion-selective electrode; however, these types of biosensor exhibit poor selectivity as well as sensitivity. In the present work, an amperometric urea biosensor using a single enzyme *i.e.* urease has been developed using a ZnO–MWCNTs hybrid nanocomposite matrix. The amperometric sensing response characteristics of the developed biosensor towards urea have been studied and compared with the bare ZnO thin film based biosensor.

2. Experimental

2.1. Chemicals and reagents

Urea and urease (Urs) (type III from jack beans) were procured from Sigma. Zinc acetate dihydrate ($C_6H_6O_4Zn\cdot 2H_2O$, 99.0%) and Triton X-100 were procured from Sigma-Aldrich (USA). Ammonia solution (25% GR) was obtained from Merck India Ltd., India. Multiwalled carbon nanotubes (MWCNTs, diameter 20–40 nm) were procured from Shenzhen Nanotech port Co., Ltd. Sodium phosphate monobasic anhydrous and sodium phosphate dibasic dihydrate were obtained from Sisco chemical, India. All chemicals were used without further purification. 50 mM phosphate buffer saline (PBS), pH 7.0 (0.9% NaCl) solution was prepared by adjusting the proportion of monobasic sodium phosphate and dibasic sodium phosphate solution (Sisco chemicals) and then adding 0.9% NaCl to the solution. Deionized (DI) water (resistivity $\sim$ 18.2 MΩ cm^{-1}) was used for the preparation of aqueous solutions. The solutions of varying concentrations of urea were prepared in DI water.

2.2. Preparation of ZnO/ITO and ZnO–MWCNT/ITO electrodes

Functionalization of MWCNTs was carried out by refluxing in a 1 : 3 v/v mixture of sulphuric acid and nitric acid followed by washing with deionized water and filtration until the pH of approximately 7.0 was reached, and they were finally dried in an oven at 60 °C.

The solutions for pure ZnO and the hybrid composite of ZnO–MWCNTs were prepared as follows. 0.455 M zinc acetate solution was prepared in DI water at room temperature. Ammonia solution (25%) was added dropwise to the above solution with constant stirring leading to the formation of a milky white precipitate (pH = 8–9). After continuous stirring for 4–5 hours at room temperature the precipitates were washed well with DI water until neutral pH = 7.0 was obtained. Subsequently, 1 M dilute HNO_3 was added yielding a transparent solution (pH = 1) of ZnO. For making the solution of hybrid ZnO–MWCNTs, the functionalized MWCNTs (0.05 and 0.1 wt%) were added to the prepared transparent ZnO sol and subsequently ultrasonicated for 6 hours. The solutions of bare ZnO and hybrid ZnO–MWCNTs composite thus obtained were spin coated on cleaned ITO coated glass slides to obtain the required matrices. In order to achieve uniform coating of the matrices (ZnO and ZnO–MWCNTs) a surfactant Triton X-100 was also added to the solutions. The process of spin coating followed by firing for 10 min. at 300 °C was repeated several times to get the desired film thickness. Finally, the prepared thin films of bare ZnO and ZnO–MWCNTs nanocomposite were annealed at 300 °C for 3 hours in order to obtain the desired crystallinity, and electrodes of ZnO/ITO and ZnO–MWCNT/ITO respectively were realized.

2.3. Immobilization of urease (Urs)

20 μl of freshly prepared urease solution (1 mg ml^{-1}, in 50 mM PBS, pH 7.0) was immobilized onto the surface of the ZnO/ITO and ZnO–CNT/ITO electrodes separately and kept for drying at room temperature. Finally, the prepared bioelectrodes of Urs/ZnO/ITO and Urs/ZnO–MWCNT/ITO were stored at 4 °C overnight. Before use, the bioelectrodes were extensively washed with phosphate buffer saline (PBS) solution to remove any

unbound enzyme from the surface. The solutions for different concentrations of urea were freshly prepared in DI water.

2.4. Experimental characterization

The structural properties of bare ZnO and hybrid composite ZnO–MWCNT thin films were studied using X-ray diffraction (XRD) [Bruker D8 Discover]. The surface morphology of the ZnO/ITO and ZnO–MWCNT/ITO electrodes was studied using scanning electron microscopy (SEM) [Quanta FEI 200]. Transmission electron microscopy (TEM) [TECHNAI G^2 T30, u-TWIN] was employed to characterize bare MWCNTs and prepared ZnO–MWCNTs nanobiocomposite. Fourier transform infrared spectroscopy (FTIR) [Perkin Elmer, Model: Frontier] was utilized to confirm the immobilization of urease onto the surface of ZnO and ZnO–MWCNTs based matrices. Cyclic voltammetric (CV) measurements were carried out on a potentiostat/galvanostat [Gamry Inc. 600] using a three-electrode electrochemical cell in PBS solution (50 mM, pH 7.0, 0.9% NaCl) containing 5 mM $[Fe(CN)_6]^{3-/4-}$ as a redox probe with Ag/AgCl as the reference electrode. The photometric assay was performed using a UV–VIS spectrophotometer [Perkin Elmer lambda 35]. For photometric measurements Urs/ZnO/ITO and Urs/ZnO–CNT/ITO bioelectrodes were dipped in a 3 ml phosphate buffer solution (50 mM, pH 7.0), containing 60 ml of Nessler's solution and 100 ml of urea solution in varying concentrations. After 2 min of incubation of the bioelectrode, absorbance of the coloured product *i.e.*, $NH_2Hg_2I_3$ (a complex formed between Nessler's reagent and ammonia produced by the enzymatic hydrolysis of urea) was formed that gives absorbance in the solution at a fixed wavelength ($\lambda = 385$ nm). This absorbance was measured at $\lambda =$ 385 nm for varying concentrations of urea to monitor the kinetics of urease immobilized on the electrode surface.

3. Results and discussion

3.1. Transmission electron microscopy (TEM) studies

Fig. 1(i) shows the TEM image of non-functionalized MWCNTs and Fig. 1((ii) and (iii)) show the images of ZnO–MWCNTs nanocomposite containing functionalized MWCNTs. The average outer diameter of the MWCNTs was found to be between 20 and 40 nm. It may be observed from Fig. 1(ii) that the functionalization decreases the weight of the MWCNTs and some defects along the side walls of the nanotubes have also occurred. The TEM image of ZnO–MWCNTs nanocomposite (Fig. 1(iii)) clearly shows that some black spots, possibly ZnO, are present in the solution and attached to different parts of the MWCNTs along their length covering the surface of the nanotubes, thus confirming the formation of the hybrid nanocomposite of ZnO and MWCNTs.

3.2. Structural and surface morphological studies

The XRD patterns obtained for the thin films of bare ZnO and hybrid nanocomposite of ZnO–MWCNTs deposited with varying MWCNTs concentrations from 0 to 0.10 wt% on glass slide are shown in ESI, Fig. 1.† The XRD patterns show reflections corresponding to (100), (002), (101), (102) and (110) crystal planes

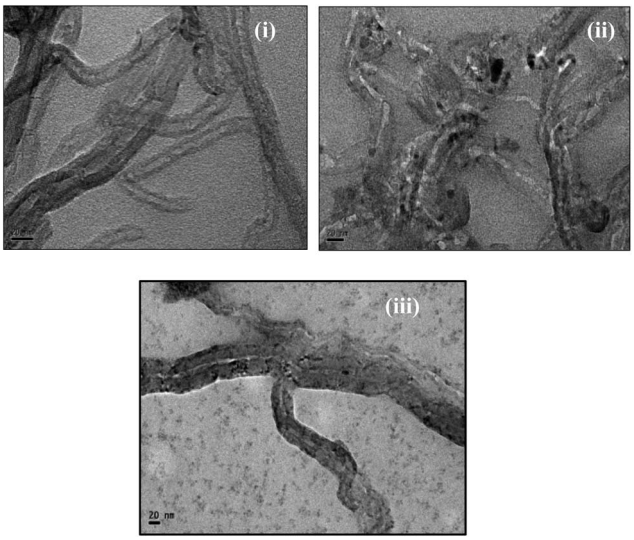

Fig. 1 TEM images of (i) bare MWCNTs, and (ii), (iii) ZnO–MWCNTs nanocomposite.

of the hexagonal wurtzite structure of ZnO indicating the growth of polycrystalline ZnO thin film.

However, a peak corresponding to the (002) plane was found to be dominating (ESI, Fig. 1†) indicating the growth of preferred oriented ZnO thin film with *c*-axis normal to the surface of the glass slide. The preferred orientation along the (002) plane was found to change with the incorporation of MWCNTs in the ZnO matrix (ESI, Fig. 1†). It can be observed from ESI, Fig. 1† that no peak corresponding to MWCNTs is visible in the XRD pattern of the ZnO–MWCNTs nanocomposite containing 0.05 wt% MWCNTs which is due to the very low concentration of incorporated MWCNTs. However, with increase in the content of MWCNTs to 0.10 wt% in the nanocomposite, a hump of very low intensity corresponding to CNTs starts appearing in the XRD pattern (ESI, Fig. 1†).

The scanning electron microscopy (SEM) images of the surface of thin films of bare ZnO and ZnO–MWCNT are shown in Fig. 2(i) and (ii). The surface morphology of bare ZnO film is found to be highly rough and nanostructured having boulder-like grains (Fig. 2(i)). An SEM micrograph of the hybrid nanocomposite matrix of ZnO–MWCNTs (Fig. 2(ii)) reveals the incorporation of MWCNTs into the ZnO matrix thus showing

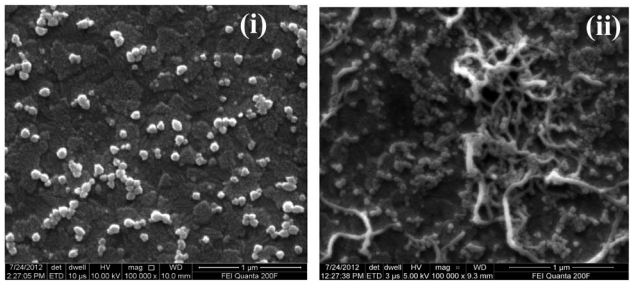

Fig. 2 SEM micrographs of the surface of (i) bare ZnO thin film and (ii) ZnO–MWCNTs hybrid nanocomposite (0.1 wt%) thin film deposited on ITO coated glass slide.

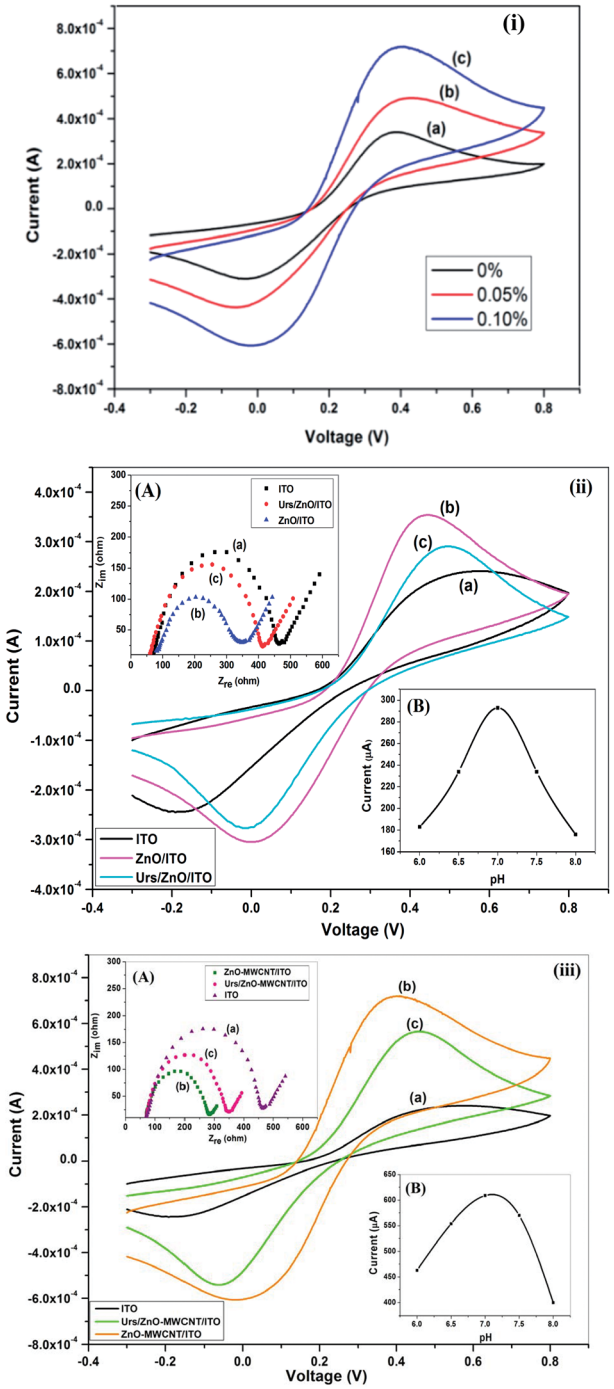

Fig. 3 (i) CV curves of ZnO–MWCNT/ITO electrodes with different MWCNTs concentrations: (a) 0 wt%, (b) 0.05 wt% and (c) 0.10 wt%, taken in PBS solution (PBS, 50 mM, pH 7.0, 0.9% NaCl) containing 5 mM $[Fe(CN)_6]^{3-/4-}$ as a redox mediator; (ii) CV curves of (a) ITO/glass, (b) ZnO/ITO electrode and (c) Urs/ZnO/ITO bioelectrode; inset (A) EIS curves of (a) ITO/glass electrode, (b) ZnO/ITO electrode and (c) Urs/ZnO/ITO bioelectrode and inset (B) CV current response of Urs/ZnO/ITO bioelectrode with varying pH of PBS solution (PBS, 50 mM, pH 7.0, 0.9% NaCl) containing 5 mM $[Fe(CN)_6]^{3-/4-}$ as a redox mediator; (iii) CV curves of (a) ITO/glass, (b) ZnO–MWCNT/ITO electrode having 0.10 wt% MWCNTs and (c) Urs/ZnO–MWCNT/ITO bioelectrode; inset (A) EIS curves of (a) ITO/glass electrode, (b) ZnO–MWCNT/ITO electrode and (c) Urs/ZnO–MWCNT/ITO bioelectrode and inset (B) CV current response of Urs/ZnO–MWCNT/ITO bioelectrode with varying pH of 50 mM PBS solution containing 5 mM $[Fe(CN)_6]^{3-/4-}$ as a redox mediator.

the formation of highly porous and rough microstructure favourable for effective immobilization of enzyme.

3.3. FTIR studies

FTIR spectroscopy was employed to confirm the immobilization of urease (Urs) onto the surfaces of ZnO and hybrid ZnO–MWCNTs (0–10 wt%) nanocomposite matrix. The FTIR spectra of both the thin films, deposited on KBr pellets under similar deposition conditions, were taken in transmission mode within the wavenumber range 380 to 4000 cm^{-1} and are shown in ESI, Fig. 2(i) and (ii)† with and without immobilization of Urs. The FTIR spectrum of bare ZnO film (ESI, Fig. 2(i)†) shows a sharp and intense absorption band centred at around 418 cm^{-1} confirming the formation of Zn–O bonds.[35] The band observed at 1600 cm^{-1} is related to the bending mode of water molecules on the surface of the sample.[36]

The FTIR spectrum after immobilization of urease over ZnO thin film (ESI, Fig. 2(i)†) shows some additional bands at 1645 cm^{-1} (corresponding to N–H stretching in amide II), 995 cm^{-1} (assigned to C–O stretching) and at 1080 cm^{-1} due to C–N vibrations[37] confirming the effective immobilization of the enzyme onto the surface of ZnO thin film. A broad band observed at around 3450 cm^{-1} is attributed to the water molecules present on the surface of the ZnO sample after enzyme immobilization (ESI, Fig. 2(i)†).

The FTIR spectrum of hybrid ZnO–MWCNTs nanocomposite is similar to that of bare ZnO thin film with some additional bands occurring at 1400 cm^{-1} due to stretching of OH bonds present in water[19] and at 2334 cm^{-1} due to the presence of atmospheric CO_2. However, due to the very low concentration of MWCNTs no absorption band related to them can be observed in the spectrum. The FTIR spectrum of the immobilized urease over ZnO–MWCNTs thin film (ESI, Fig. 2(ii)†) shows similar absorption bands to those observed earlier in the case of urease on bare ZnO film (ESI, Fig. 2(i)†). The results confirm the effective loading of immobilized urease on the surface of ZnO and ZnO–MWCNTs nanocomposite thin film matrices by the physical adsorption technique.

3.4. Electrochemical studies

3.4.1. Electrochemical impedance spectroscopy (EIS) studies. Insets (A) of Fig. 3(ii) and (iii) show the electrochemical impedance spectroscopy (EIS) spectra for the ZnO/ITO and ZnO–MWCNT/ITO electrodes respectively recorded in PBS buffer (PBS, 50 mM, pH 7.0, 0.9% NaCl) containing 5 mM $[Fe(CN)_6]^{3-/4-}$. Different curves in Fig. 3(i) and (ii) show the EIS spectra of ITO coated glass platform (curve (a)); ZnO or ZnO–CNT nanocomposite thin films coated on ITO coated glass (curve (b)) and urease immobilized on the respective thin film matrices (curve (c)). Well defined EIS spectra were obtained for all prepared electrodes, and the corresponding values of charge transfer resistance (R_{CT}) are listed in ESI, Table 1.† The presence of ZnO or ZnO–MWCNTs nanocomposite matrix on the ITO surface results in a significant decrease in the value of electron-transfer resistance R_{CT} (curve (b) in inset (A) of Fig. 3(ii) and (iii)). The obtained results indicate that the prepared thin film

matrix of ZnO or ZnO–MWCNTs nanocomposite has induced rapid electron communication that results in enhanced electron transfer kinetics of the electrode. Furthermore, it may be noted from ESI, Table 1† that the R_{CT} value for the ZnO–MWCNT/ITO electrode (208.32 Ω) is less compared to the corresponding value (273.00 Ω) obtained for the ZnO/ITO electrode. This is attributed to the fact that the MWCNTs incorporated into the ZnO matrix provide a short conducting path and thus result in an increase in electrical conductivity, hence offering lesser resistance to the charges for communication.[36] However for both the electrodes, the value of R_{CT} increases on enzyme immobilization (curve (c) in inset (A) of Fig. 3(ii) and (iii)), and is attributed to the insulating nature of immobilized urease which hinders the flow of charge carriers between the PBS solution and the electrode (ESI, Table 1†).

3.4.2. Cyclic voltammetric (CV) studies. Fig. 3(i) shows the CV curves of the ZnO–MWCNT/ITO electrodes having different concentrations of MWCNTs (0 to 0.10 wt%). The curves were obtained in PBS solution containing 5 mM $[Fe(CN)_6]^{3-/4-}$, which act as an external mediator for providing the redox couple. All the CV curves show well defined oxidation and reduction peaks (Fig. 3). The peak oxidation current is found to be increasing continuously with an increase in the concentration of incorporated MWCNTs, having a value of about 0.72 mA for ZnO–MWCNTs nanocomposite electrode having 0.10 wt% MWCNTs. This is related to an increase in the conductivity of the composite matrix with incorporation of more MWCNTs. The peak oxidation current of the nanocomposite matrix is found to increase with further increasing the content of MWCNTs (>0.10 wt%) in the composite matrix; however, MWCNTs are seen to be leaching out of the electrode and settle down in the buffer solution, resulting in an unstable CV response. Therefore, ZnO–MWCNT/ITO nanocomposite electrode having 0.10 wt% of MWCNTs was used for carrying out further experiments. Fig. 3(ii) and (iii) show the CV curves obtained for ZnO/ITO and ZnO–MWCNT/ITO electrodes at a scan rate of 100 mV s^{-1}. The peak oxidation current was found to increase from around 0.24 mA to 0.35 mA after integration of ZnO thin film with ITO surface (Fig. 3(ii), curve (a) and (b)) which may be due to the good electron communication feature of the deposited ZnO thin film. However, a much higher increase in peak oxidation current (0.72 mA) was observed for ZnO–MWCNT/ITO electrode (curve (b), Fig. 3(iii)) due to improved electrical conductivity of the hybrid nanocomposite electrode. The obtained results are in agreement with the EIS studies discussed earlier. The immobilization of non-conducting enzyme on the surface of both ZnO/ITO and ZnO–MWCNT/ITO electrodes results in a decrease in peak oxidation current along with an increase in the peak-to-peak separation of the redox potential (curve (c) in Fig. 3(ii) and (iii)). The observed increase in peak-to-peak potential is because of some potential drop occurring across the immobilized urease on the surface of electrodes, which is of insulating nature. Insets (B) in Fig. 3(ii) and (iii) show the variation of peak oxidation current with varying pH of PBS solution for Urs/ZnO/ITO and Urs/ZnO–MWCNT/ITO bioelectrodes respectively. It can be observed that for both the bioelectrodes, maximum peak oxidation current is obtained at a pH of 7.0, where the biomolecule retains its natural structure and does not become denatured thus giving maximum activity. Hence, the pH of the PBS buffer solution was maintained at 7.0 for all further measurements.

In order to estimate the surface concentration of the ionic species on the surface of Urs/ZnO/ITO and Urs/ZnO–MWCNT/ITO bioelectrodes, CV curves as a function of scan rate (υ) were recorded for both the bioelectrodes and are shown in Fig. 4(i) and (ii) respectively.

For both the bioelectrodes, the oxidation (I_{po}) as well as the reduction (I_{pr}) peak currents vary linearly with the square root of scan rate ($\upsilon^{1/2}$) (insets (A) in Fig. 4(i) and (ii)), suggesting that the redox process of immobilized urease on the surface of ZnO and ZnO–MWCNTs bioelectrodes follows diffusion controlled kinetics.[37] It was also found that as the scan rate increases, both the oxidation and reduction peak currents increase along with

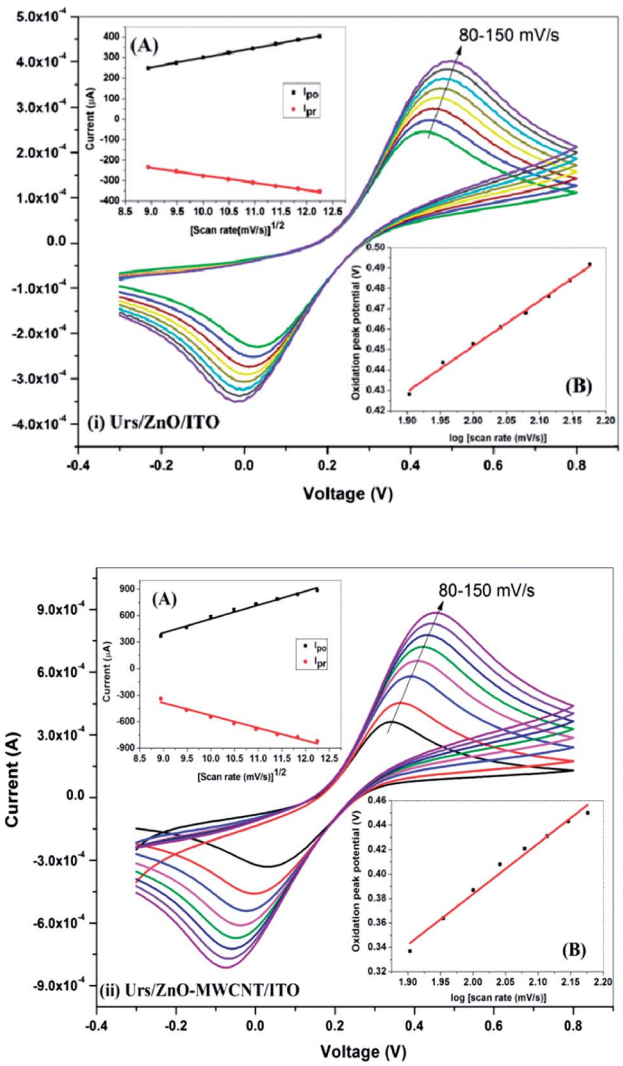

Fig. 4 CV curves of the (i) Urs/ZnO/ITO and (ii) Urs/ZnO–MWCNT/ITO bioelectrodes at scan rates varying from 80 to150 mV s^{-1} recorded in PBS solution (PBS, 50 mM, pH 7.0, 0.9% NaCl) containing 5 mM $[Fe(CN)_6]^{3-/4-}$ as a redox mediator. Insets: (A) plot of peak oxidation (I_{po}) and reduction (I_{pr}) currents as a function of the square root of scan rate and (B) plot of oxidation peak potential as a function of the logarithm of scan rate.

an appreciable shift in the oxidation peak towards higher potential and of the reduction peak towards lower potential (insets (B) in Fig. 4(i) and (ii)) implying the quasi-reversibility of the system.[39]

The surface concentration (Γ) of ionic species per unit area of the enzyme for both the bioelectrodes was estimated by using the Brown–Anson model.[40] The estimated values of Γ for Urs/ZnO/ITO and Urs/ZnO–MWCNT/ITO bioelectrodes are found to be 1.08×10^{-8} mol cm^{-2} and 1.88×10^{-7} mol cm^{-2} respectively which are much higher than the corresponding values reported in literature for urea biosensors.[4] The higher value of Γ obtained for the hybrid ZnO–MWCNTs nanocomposite matrix based bioelectrode clearly indicates higher loading of urease on the surface of the nanostructured composite matrix in comparison to that on the bare ZnO matrix based bioelectrode.

3.4.3. Electrochemical sensing response. Fig. 5(i) and (ii) show the cyclic voltammograms obtained for Urs/ZnO/ITO and Urs/ZnO–MWCNT/ITO bioelectrodes respectively as a function of urea concentration. It can be noted from Fig. 5(i) and (ii) that the peak oxidation current gradually increases with increase in urea concentration from 0 to 100 mg dl^{-1} for both the bioelectrodes. The increase in the oxidation current is due to enhanced biochemical reaction taking place on the bioelectrode surface with increasing analyte concentration (urea). The urea biosensor response without immobilization of enzyme (urease) was also investigated by carrying out a control experiment in which sensing response for urea was studied without immobilization of urease on the surface of ZnO–MWCNT/ITO electrode. It was found that no change in the redox peak currents was observed in the cyclic voltammograms for the ZnO–MWCNT/ITO electrode upon addition of different urea concentrations from 0 to 100 mg dl^{-1} to the $K_3[Fe(CN)_6]$ mediated phosphate buffer saline (PBS) solution indicating that the oxidation of urea does not occur at the surface of the transducer (ZnO–MWCNTs/ITO) without immobilizing enzyme. Thus, the increase in CV oxidation current observed in the biosensing reaction involving Urs/ZnO–MWCNTs/ITO bioelectrodes with varying urea concentrations of urea is solely due to the bioelectrocatalytic oxidation of urea in the presence of immobilized urease and not due to the direct oxidation of urea on the surface of ZnO–MWCNTs/ITO electrode. The observed results confirm that enzyme (urease) plays a significant role as an electrocatalyst in the present study and the hybrid matrix of ZnO–MWCNTs provides an efficient platform for conformal immobilization of urease.

The schematic of the possible biochemical reactions occurring at the surface of the prepared bioelectrode is shown in Scheme 1. In PBS solution containing 5 mM $[Fe(CN)_6]^{3-/4-}$ as the redox mediator species, analyte (urea) of different concentrations is added which upon oxidation in the presence of immobilized urease gives rise to chemical products like ammonia (NH_3) and carbon dioxide (CO_2), and subsequently during this reaction the urease gets reduced. The activity of urease is due to the presence of SH groups on its active site that can be oxidized as well as reduced by the biochemical reactions.[41] Hence, the reduced urease loses electrons and gets oxidized. The Fe^{3+} ions present in the PBS solution as a result of $[Fe(CN)_6]^{3-/4-}$ redox mediator species capture the released

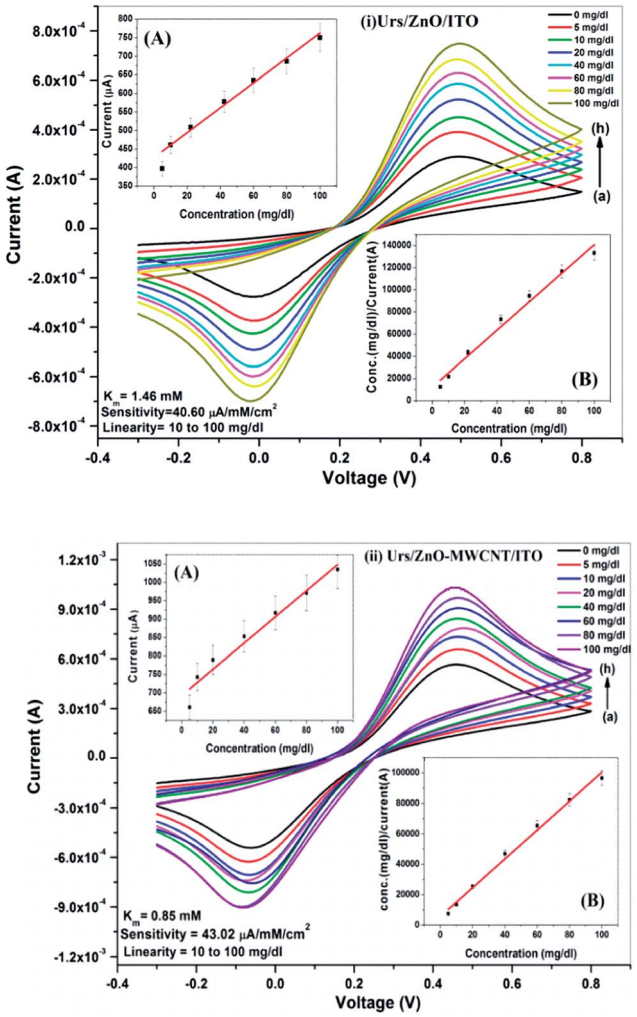

Fig. 5 Electrochemical response of (i) Urs/ZnO/ITO and (ii) Urs/ZnO–MWCNT/ITO bioelectrodes as a function of urea concentration (in mg dl^{-1}): (a) 0, (b) 5, (c) 10, (d) 20, (e) 40, (f) 60, (g) 80, (h) 100 obtained in PBS solution (PBS, 50 mM, pH 7.0, 0.9% NaCl) containing 5 mM $[Fe(CN)_6]^{3-/4-}$ as a redox mediator. Insets: (A) calibration curve variation of peak oxidation current as a function of urea concentration and (B) Hanes plot to determine Michaelis–Menten constant (K_m).

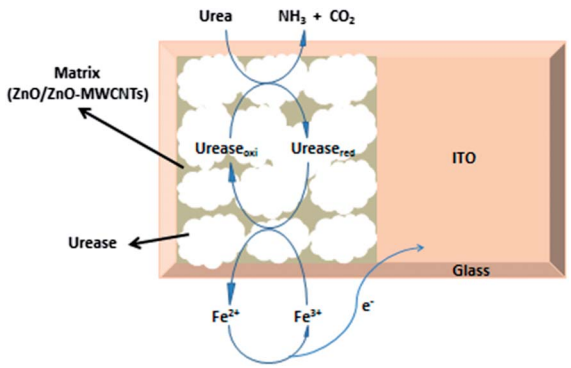

Scheme 1 Schematic of the electron transfer process occurring at the surface of the bioelectrode (top view) in the presence of $[Fe(CN)_6]^{3-/4-}$ redox species.

electrons in the vicinity of the bioelectrode surface and reduces to Fe^{2+} ions. Further, when Fe^{2+} ions oxidize back to Fe^{3+} ions the released electrons are transferred to the underneath ITO layer of the bioelectrode *via* an efficient matrix (ZnO or ZnO–MWCNTs) possessing fast electron communication feature and thus completing the conduction path. The above discussed electron transfer process takes place during the forward scan of the voltammograms and during the reverse scan the whole process gets repeated in the opposite manner as shown in Scheme 1.

Hence, the catalytic oxidation of urea by the immobilized urease involves gain or loss of electrons thus completing a redox reaction and the observed increase in the oxidation peak current with increasing concentration of urea (Fig. 5) is attributed to the increase in the number of released electrons during oxidation.

Insets (A) in Fig. 5(i) and (ii) show the variation of peak oxidation current with the uric acid concentration for the Urs/ZnO/ITO and Urs/ZnO–MWCNT/ITO bioelectrodes respectively. It can be seen from Fig. 5(i) and (ii) that the magnitude of the peak oxidation current increases linearly from 0.30 mA to 0.75 mA and from 0.57 mA to 1.04 mA with increase in the urea concentration from 0 to 100 mg dl^{-1} for ZnO and ZnO–MWCNTs matrix based bioelectrodes respectively. The calibration curves obtained for Urs/ZnO/ITO and Urs/ZnO–MWCNT/ITO bioelectrodes have been fitted to the linear regression equations (1) and (2) respectively and are given as follows:

$$\text{Current } (\mu A) = 3.35\ (\mu A) \times \text{urea concentration (mg dl}^{-1}) + 426.89;\ R = 0.996 \quad (1)$$

and,

$$\text{Current } (\mu A) = 3.55\ (\mu A) \times \text{urea concentration (mg dl}^{-1}) + 692.92;\ R = 0.998 \quad (2)$$

where R is the linear regression coefficient having value >0.99 in the present study. The linear enhancement in the peak oxidation current with increase in urea concentration suggests that both ZnO and ZnO–MWCNTs matrices provide favourable microenvironment to the immobilized enzyme. The sensitivities for ZnO and ZnO–MWCNTs nanocomposite based biosensors are about 40.6 μA mM^{-1} cm^{-2} and 43.0 μA mM^{-1} cm^{-2} respectively, which are much higher than the corresponding values reported in literature.[4,19,40–43] It is important to note that the bioelectrode based on hybrid ZnO–MWCNTs nanocomposite matrix offers better sensitivity in comparison to that of pure ZnO thin film and is attributed to enhanced electron communication feature due to incorporation of MWCNTs in the ZnO matrix. The detection limits (DL) for the bioelectrodes have been calculated using the following expression:

$$DL = (3 \times SD)/S$$

where SD is the standard deviation in peak oxidation current and S is the sensitivity of the electrode towards urea. The detection limits of urea are found to be about 0.23 mM (~1.43 mg dl^{-1}) and 0.30 mM (~1.86 mg dl^{-1}) for Urs/ZnO–MWCNT/ITO and Urs/ZnO/ITO bioelectrodes respectively, which are much lower than correspondingly reported values by other workers.[43] It is important to highlight that all the experiments were carried out in triplicate sets on the same electrodes and different electrodes fabricated under similar conditions and the obtained results reveal reproducibility of the system within 3% error.

The apparent Michaelis–Menten constant (K_m), which gives an indication about the enzyme–analyte kinetics, is obtained from the Hanes plot[37] as shown in insets (B) of Fig. 5(i) and (ii) for the Urs/ZnO/ITO and Urs/ZnO–MWCNT/ITO bioelectrodes respectively. It is known that the value of K_m is dependent strongly on the nature of the matrix that often exhibits favourable conformational changes in the immobilized enzyme.[37] In the present work, estimated values of K_m for the Urs/ZnO/ITO and Urs/ZnO–MWCNT/ITO bioelectrodes are found to be about 1.45 mM and 0.85 mM respectively. If an enzyme has a small value of K_m, it achieves its maximum catalytic efficiency at low analyte concentrations. Hence, the smaller the value of K_m, the more efficient is the adsorbed catalyst. The value of K_m for bare ZnO based bioelectrode is about 1.46 mM whereas for ZnO–MWCNTs nanocomposite based bioelectrode it is about 0.85 mM. The low value of K_m indicates that the electrode containing MWCNTs exhibits fast biochemical reaction kinetics and would have its maximum catalytic efficiency at very low urea concentration. The obtained results clearly show the effectiveness of MWCNTs in increasing the electrocatalytic efficiency of the enzyme which may be attributed to the suitable microenvironment provided by the incorporated multiwalled carbon nanotubes in the ZnO–MWCNTs nanocomposite matrix for immobilizing urease with proper conformation and orientation. The value of K_m obtained in the present work for the hybrid nanocomposite based matrix is much lower in comparison to that of the pure ZnO matrix as well as already reported values in literature[19,42] indicating a higher affinity of immobilized urease towards urea which may be attributed to the fact that presence of MWCNTs in the nanocomposite provides larger surface to volume ratio for enzyme immobilization besides introducing favourable conformational changes. Also, the electron communication rate is enhanced by providing a short conducting path across the grain boundaries of ZnO in the hybrid nanocomposite (ZnO–MWCNTs) matrix,[38] thus increasing the rate of biochemical reaction between the immobilized urease and analyte which is an essential criterion for developing an efficient urea biosensor. Thus, the ZnO–MWCNTs nanocomposite thin film based matrix offers a better platform for enzyme immobilization over a bare ZnO thin film based matrix for biosensing applications.

3.5. Photometric assay

The prepared bioelectrodes were incubated for 2 minutes in 3 ml of PBS solution (pH 7.0) containing 60 μl of Nessler's reagent and 100 μl of urea in varying concentration from 0.83 to 16.65 mM (*i.e.* 5–100 mg dl^{-1}). The differences between the values of initial and final absorbance measured at a fixed wavelength ($\lambda = 385$ nm) as a function of urea concentration are plotted in Fig. 6 for both the bioelectrodes.

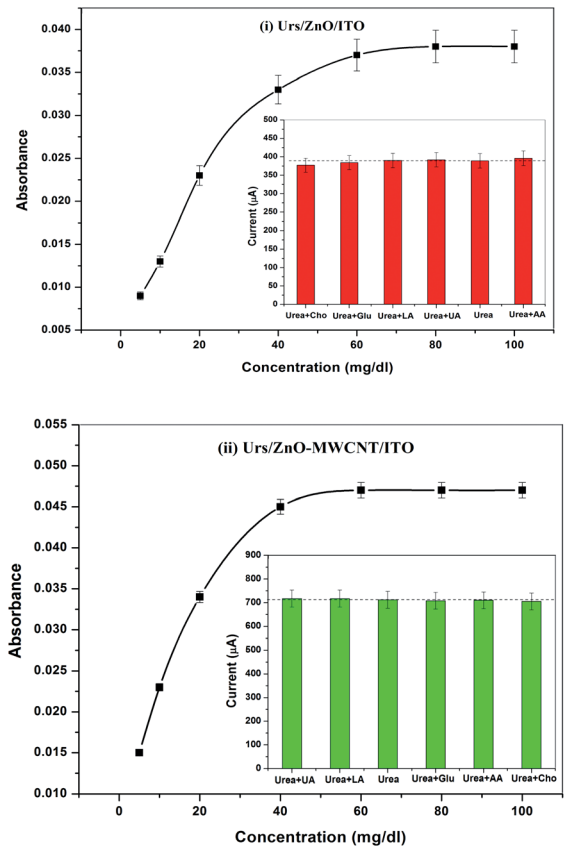

Fig. 6 Photometric assay as a function of urea concentration and insets show the effect of interferents for (i) Urs/ZnO/ITO bioelectrode and (ii) Urs/ZnO–MWCNT/ITO bioelectrode.

A similar trend in the variation of absorbance values has been observed for both the bioelectrodes which initially increases with increase in urea concentration and thereafter attains a saturation value. The apparent enzyme activity, *i.e.* the amount of enzyme bound onto the bioelectrode surface, has been calculated using the equation ${}^{enz}a_{app}$ (U cm^{-2}) = $AV/\varepsilon ts$, where A is the difference in absorbance before and after bioelecrode incubation, V is the total volume (3.17 cm^3), ε is the millimolar extinction coefficient of Nessler's reagent, t is the reaction time (2 min) and s is the surface area of the electrode (0.25 cm^2). The estimated value of the apparent enzyme activity for the ZnO thin film based bioelectrode is calculated to be 2.20 $\times$ 10^{-2} U cm^{-2} whereas for ZnO–MWCNTs nanocomposite based bioelectrode it is about 2.73 $\times$ 10^{-2} U cm^{-2}. The high activity of the immobilized Urs on the surface of the hybrid ZnO–MWCNTs nanocomposite matrix compared to that on the bare ZnO thin film matrix is attributed to the nanostructured morphology due to the incorporation of MWCNTs in ZnO. The obtained results in the present work are much better than those reported in literature for ZnO based biosensors.[24,46]

3.6. Selectivity and shelf-life studies

The effect of inteferents on the prepared bioelectrodes was tested by cyclic voltammetric technique. In this experiment the effects of a number of metabolites other than urea which are present in human blood/serum, such as cholesterol (Cho) (5 mM), glucose (Glu) (5 mM), uric acid (UA) (0.1 mM), ascorbic acid (AA) (0.1 mM) and lactic acid (LA) (0.5 mM) that may produce interference in the biosensing response of the bioelectrode towards urea, were studied. The selectivity studies of the bioelectrode was carried out by monitoring the cyclic voltammograms (CV) obtained after the addition of various interferents separately to the $K_3[Fe(CN)_6]$ mediated PBS solution containing 1 mM of urea. For example, cyclic voltammograms obtained after the interference study of cholesterol and uric acid are shown in ESI, Fig. 3† and it can be seen that the behaviour of CV for both the bioelectrodes remains almost the same after the addition of these interferents. The peak oxidation currents obtained after the addition of various interferents are shown in the bar graphs (insets of Fig. 6(i) and (ii)). The amount of interference was calculated according to eqn (3):

$$\text{Interference } (\%) = (|I_i - I_u|/I_u) \times 100 \quad (3)$$

where I_i and I_u are the peak oxidation currents recorded in solutions containing interferent mixed with urea and urea alone respectively. The obtained results clearly demonstrate that the presence of various interferents has a negligible effect on the biosensing response of both Urs/ZnO/ITO and Urs/ZnO–MWCNT/ITO bioelectrodes towards urea with only 0.7% and 3.0% of maximum interference from cholesterol for Urs/ZnO–MWCNT/ITO and Urs/ZnO/ITO bioelectrodes respectively. Thus, it is inferred that the prepared bioelectrode based on the ZnO–MWCNTs thin film is capable of highly selective determination of urea. The results are much better than those reported in literature on urea biosensors using other metal oxide based matrices.[4] The stability of the biosensor is determined by its shelf-life study. The CV response is measured at a fixed concentration (60 mg dl^{-1}) of urea after a regular interval of time (~1 week) for both Urs/ZnO/ITO and Urs/ZnO–MWCNT/ITO bioelectrodes. It may be noted that the CV responses for both the bioelectrodes (ESI, Fig. 4(i) and (ii)†) were found to remain almost the same while retaining their proper shape for up to 14 weeks of storage in the case of Urs/ZnO/ITO and 16 weeks of storage in the case of Urs/ZnO–MWCNT/ITO bioelectrode. Also, the activities of both the bioelectrodes are very high (88% for Urs/ZnO/ITO and 92% for Urs/ZnO–MWCNT/ITO bioelectrode) after several weeks of storage at 4 °C. The obtained CV responses are in support of the long term stability of the fabricated biosensor which is much higher than the earlier reported values of shelf-life for electrochemical biosensors based on ZnO–CNT electrodes.[30,31] This may be due to the fact that the presently fabricated ZnO–MWCNTs nanocomposite based electrode offers high effective surface area for enzyme immobilization and results in higher amount of enzyme loading onto the electrode surface. In addition to this, in the present work a very suitable microenvironment for the enzyme immobilization with favourable conformation is provided by the ZnO–MWCNTs hybrid nanocomposite which preserves the natural activity of the enzyme and helps in long term stability of

Table 1 A comparative study of metal oxide based amperometric urea biosensors

Matrix	Detection range (mM)	Detection limit (mM)	Sensitivity ($\mu A\ mM^{-1}\ cm^{-2}$)	Response time (s)	Shelf-life (weeks)	Ref.
ZnO thin film	0.8–13.3	2.24	8.7	—	—	19
ZnO–chitosan composite	0.8–16.6	0.49	0.13	10	12	42
Chitosan–Fe_3O_4 composite	0.8–16.6	0.33	12.50	10	8	43
ZrO_2 thin film	0.8–16.6	0.8	0.07	10	16	44
TiO_2–ZrO_2 composite	0.8–16.6	0.44	2.74	10	—	45
ZnO–MWCNTs composite	0.8–16.6	0.23	43.02	4	>16	Present work

Table 2 Determination of urea in human serum samples using the proposed biosensor

Real serum sample number	Concentration of urea measured ($mg\ dl^{-1}$)		RSD of developed biosensor ($n = 5$) (%)
	Urs/ZnO–MWCNT/ITO bioelectrode (present work)	Spectrophotometric method (pathlab report)	
1	24.1	24.0	1.1
2	26.7	27.0	1.0
3	29.0	30.0	2.1
4	47.6	48.0	2.4
5	75.1	74.0	1.2

the urea biosensor. The biosensing results obtained for both the bioelectrodes (Urs/ZnO/ITO and Urs/ZnO–MWCNT/ITO) are summarized in ESI, Table 2.

It may be clearly seen from ESI, Table 2† that the hybrid nanocomposite based bioelectrode exhibits better biosensing response characteristics towards urea in comparison to the pure ZnO thin film matrix based bioelectrode exhibiting a higher sensitivity (43.0 $\mu A\ mM^{-1}\ cm^{-2}$), low K_m value (0.85 mM), high shelf-life (retains 92% of activity even after 16 weeks), high surface coverage (1.88×10^{-7} mol cm^{-2}) and an enhanced enzyme activity (2.73×10^{-2} units per cm^2). The results are much better than the corresponding values reported in literature for amperometric urea biosensors using metal oxide based matrices and are tabulated in Table 1.[19,43–45]

To demonstrate the feasibility of the developed Urs/ZnO–MWCNT/ITO biosensor for the analysis of urea in human serum, five real samples were analysed and the % RSD values were calculated. In order to determine the urea concentration in real serum, CV analysis was performed to obtain the peak oxidation current in the same way as for the urea solution and the concentration of urea peak oxidation was interpolated from the calibration curve. To validate the accuracy of the fabricated urea biosensor, the content of urea in serum samples determined by the biosensor was compared with that measured by the commercial spectrophotometric method in the path laboratory. Table 2 summarizes the results obtained during the present investigation. The obtained values of concentration of urea in all serum samples using the developed biosensor are found to be in good agreement with the corresponding data obtained from spectrophotometric methods indicating the applicability of the prepared biosensor for efficient detection of urea.

4. Conclusions

In summary, chemically deposited bare ZnO and hybrid ZnO–MWCNTs nanocomposite matrices have been exploited successfully for the realization of Urs/ZnO/ITO and Urs/ZnO–MWCNT/ITO bioelectrodes for efficient detection of urea. The ZnO–MWCNTs nanocomposite matrix shows promising results in comparison to the bare ZnO matrix as it offers a large surface area for effective enzyme immobilization with better conformation. Furthermore, the incorporation of MWCNTs in ZnO provides short conducting paths across the ZnO grain boundaries thereby offering high electronic conductivity. The Urs/ZnO–MWCNT/ITO nanobioelectrode exhibits good linearity over a wide range of urea concentration (10–100 $mg\ dl^{-1}$), high sensitivity (42.0 $\mu A\ mM^{-1}\ cm^{-2}$), low value of K_m (0.85 mM), and a low detection limit of about 0.23 mM (*i.e.* 1.43 $mg\ dl^{-1}$). Results obtained in the present work are encouraging and pave the way towards the realization of other useful biosensors utilizing a very useful ZnO–MWCNTs nanocomposite in future.

Acknowledgements

Authors are thankful to Department of Science and Technology (DST), Govt. of India for the financial support to carry out this work. One of the authors (MT) is thankful to UGC for the research fellowship.

Notes and references

1 A. J. Taylor and P. Vadgama, *Ann. Clin. Biochem.*, 1992, **29**, 24.
2 L. D. Ciana and G. Caputo, *Clin. Chem.*, 1996, **42**, 1079.
3 G. Dhawan, G. Sumana and B. D. Malhotra, *Biochem. Eng. J.*, 2009, **44**, 42.

4 M. Tyagi, M. Tomar and V. Gupta, *Biosens. Bioelectron.*, 2013, **41**, 110.
5 R. V. Bisht, W. Takashima and K. Kaneto, *Biomaterials*, 2005, **26**, 3683.
6 J. V. D. Melo, S. Cosnier, C. Mousty, C. Martelet and N. J. Renault, *Anal. Chem.*, 2002, **74**, 4037.
7 N. Batra, M. Tomar and V. Gupta, *Analyst*, 2012, **137**, 5854.
8 W. J. Cho and H. J. Huang, *Anal. Chem.*, 1998, **70**, 3946.
9 B. Lakard, G. Herlem, S. Lakard, A. Antoniou and B. Fahys, *Biosens. Bioelectron.*, 2004, **19**, 1641.
10 A. Sehitogullari and A. H. Uslan, *Talanta*, 2002, **57**, 1039.
11 S. Marcos, R. Hortigiiela, J. Galbfin, J. R. Castillo and O. S. Wolfbeis, *Microchim. Acta*, 1999, **130**, 267.
12 S. B. Adeloju, S. J. Shaw and G. G. Wallace, *Anal. Chim. Acta*, 1993, **281**, 611.
13 E. Prats-Alfonso, L. Abad, N. Casañ-Pastor, J. Gonzalo-Ruiz and E. Baldrich, *Biosens. Bioelectron.*, 2013, **39**, 163.
14 A. Tiwari, S. Aryal, S. Pilla and S. Gong, *Talanta*, 2009, **78**, 1401.
15 H. C. Tsai, R. A. Doong, H. C. Chiang and K. T. Chen, *Anal. Chim. Acta*, 2003, **481**, 75.
16 R. Sahney, S. Ananda, B. K. Puri and A. K. Srivastava, *Anal. Chim. Acta*, 2006, **578**, 156.
17 A. Zhang, Y. Hou, N. Jaffrezic-Renault, J. Wan, A. Soldatkin and J. M. Chovelon, *Bioelectrochemistry*, 2002, **56**, 157.
18 M. U. Ali, N. H. Alvi, Z. Ibupoto, O. Nur, M. Willander and B. Danielsson, *Sens. Actuators, B*, 2011, **152**, 241.
19 A. Ali, A. A. Ansari, A. Kaushik, P. R. Solanki, A. Barik, M. K. Pandey and B. D. Malhotra, *Mater. Lett.*, 2009, **63**, 2473.
20 S. G. Ansari, Z. A. Ansari, H. K. Seo, G. S. Kim, Y. S. Kim, G. Khang and H. S. Shin, *Sens. Actuators, B*, 2008, **132**, 265.
21 T. Suzuki, I. Kosacki and H. U. Anderson, *J. Am. Ceram. Soc.*, 2004, **84**, 2007.
22 F. E. Ghodsi, F. Z. Tepehan and G. G. Tepehan, *Electrochim. Acta*, 1999, **44**, 3127.
23 A. B. Djurišić, X. Chen, Y. H. Leunga and A. M. C. ng, *J. Mater. Chem.*, 2012, **22**, 6526.
24 S. Saha and V. Gupta, *J. Appl. Phys.*, 2011, **110**, 064904.
25 S. Saha, S. K. Arya, S. P. Singh, K. Sreenivas, B. D. Malhotra and V. Gupta, *Biosens. Bioelectron.*, 2009, **24**, 2040.
26 Q. Ruia, K. Komorib, Y. Tiana, H. Liua, Y. Luoa and Y. Sakai, *Anal. Chim. Acta*, 2010, **670**, 57.
27 N. Zhou, J. Li, H. Chen, C. Liao and L. Chen, *Analyst*, 2013, **138**, 1091.
28 N. Zhou, H. Chen, J. Li and L. Chen, *Microchim. Acta*, 2013, **180**, 493.
29 D. Odaci, A. Telefoncu and S. Timur, *Sens. Actuators, B*, 2008, **132**, 159.
30 C. Zhang, G. Wang, M. Liu, Y. Feng, Z. Zhang and B. Fang, *Electrochim. Acta*, 2010, **55**, 2835.
31 B. Fang, C. Zhang, W. Zhang and G. Wang, *Electrochim. Acta*, 2009, **55**, 178.
32 S. Palanisamy, S. Cheemalapati and S. M. Chen, *Anal. Biochem.*, 2012, **429**, 108.
33 Y. T. Wang, L. Yu, J. Wang, L. Lou, W. J. Du, Z. Q. Zhu, H. Peng and J. Z. Zhu, *J. Electroanal. Chem.*, 2011, **661**, 8.
34 B. Haghighi and S. Bozorgzadeh, *Talanta*, 2011, **85**, 2189.
35 R. Gopikrishnan, K. Zhang, P. Ravichandran, S. Baluchamy, V. Ramesh, S. Biradar, P. Ramesh, J. Pradhan, J. C. Hall, A. K. Pradhan and G. T. Ramesh, *Nano-Micro Lett.*, 2010, **2**, 31.
36 M. Ludvigsson, J. Lindgren and J. Tegenfeldt, *Electrochim. Acta*, 2000, **45**, 2267.
37 K. Jindal, M. Tomar and V. Gupta, *Biosens. Bioelectron.*, 2012, **38**, 11.
38 A. Sharma, M. Tomar and V. Gupta, *J. Mater. Chem.*, 2012, **22**, 23608.
39 K. Arora, M. Tomar and V. Gupta, *Biosens. Bioelectron.*, 2011, **30**, 333.
40 M. Tyagi, M. Tomar and V. Gupta, *Anal. Chim. Acta*, 2012, **726**, 93.
41 S. Uchiyama, M. Kobayashi and Y. Hasebe, *Electroanalysis*, 2002, **14**, 1644.
42 P. R. Solanki, A. Kaushik, A. A. Ansari, G. Sumana and B. D. Malhotra, *Appl. Phys. Lett.*, 2008, **93**, 163903.
43 A. Kaushik, P. R. Solanki, A. A. Ansari, G. Sumana, S. Ahmad and B. D. Malhotra, *Sens. Actuators, B*, 2009, **138**, 572.
44 G. Sumana, M. Das, S. Srivastava and B. D. Malhotra, *Thin Solid Films*, 2010, **519**, 1187.
45 S. Srivastava, A. Ali, P. R. Solanki, P. M. Chavhan, M. K. Pandey, A. Mulchandani, A. Srivastava and B. D. Malhotra, *RSC Adv.*, 2013, **3**, 228.
46 S. Saha, V. Gupta, K. Sreenivas, H. H. Tan and C. Jagadish, *Appl. Phys. Lett.*, 2010, **97**, 133704.